Nuclear Instruments and Methods in Physics Research B9 (1985) 209–217
North-Holland, Amsterdam

AN APPROXIMATE ANALYTICAL CALCULATION OF PRECIPITATE DISSOLUTION RATE USING A SLOWING DOWN-DIFFUSION THEORY FOR CHARGED PARTICLES

Philip CHOU and Nasr M. GHONIEM

School of Engineering and Applied Science, University of California at Los Angeles, Los Angeles, CA 90024, USA

Received 6 December 1984

The dynamic dissolution of microstructures by radiation induced collision cascades is theoretically calculated. Coupled cascade-slowing down diffusion equations are formulated. The resulting equations are decoupled and analytically solved by using the Neumann series expansion for total particle fluxes. Specific examples illustrating the dependence of precipitate dissolution rate on its size and the incident PKA energy are given. Spatial fluxes and currents of precipitate and matrix atoms are calculated. Dissolution parameters which control the stability of precipitates show that the concept of a modified "escape zone" for precipitate atoms from its surface is a valid representation of the phenomenon. It is shown that, for large precipitates, the dissolution rate is approximately proportional to the incident ion energy and inversely proportional to the precipitate radius.

1. Introduction

The evolution of microstructural features during irradiation involves complex physical phenomena. Dynamic, diffusional and microchemical processes cooperate synergistically to produce changes in the properties of these features. Atomic diffusional processes can now be adequately modeled by the rate theory of chemical kinetics. Microchemical changes during irradiation are more complex to describe, but can be accounted for by using chemical thermodynamics. However, the effects of radiation on microstructural features through dynamic collisions is a relatively unexplored area. Neutron or ion collisions with materials create PKA's (primary knock-on atoms) which in turn lead to atomic displacements. Average energy PKA's emerging from collisions with high energy neutrons, or fast ions, can cause atomic displacements on the order of a few thousands. It is therefore conceivable that if these displacements lead to the ejection of precipitate atoms into the matrix, precipitates would be unstable under irradiation. Balance between microstructural processes, such as dissolution due to high energy collision events and re-formation rate by atomic diffusion, eventually control precipitate stability [1,2].

The strength of dynamic dissolution processes can be measured by a dissolution parameter. This can be defined as the ratio of precipitate atomic ejection rate to matrix displacement rate. When this ratio is unity, every displacement of a precipitate atom leads to its permanent implantation into the matrix. This process is, in a way, similar to atomic displacements. However, the energy involved in a dissolution event is much higher than the displacement energy, due to the fact that energies are required for the displacement of precipitate atoms as well as the transport of those atoms into the matrix. Therefore, it is expected that such long-range displacement events are much more difficult as compared to traditional atomic displacement events. In an earlier paper [3], we developed a Monte Carlo computer program, TRIPOS, to study the *TR*ansport of *I*ons in *PO*lyatomic *S*olids. The interaction between collision cascades and precipitates was numerically stimulated. In this paper, an approximate analytical theory is developed for the study of the dynamic interaction between primary knock-on atoms (PKA's) and microstructural features. A diffusion formulation, derived from transport theory, is given. Coupled particle slowing-diffusion equations are solved by expanding the flux in Neumann series. The dissolution parameter is evaluated based upon an average PKA generated from neutrons at different energies. Finally, an empirical formula for the dissolution parameter is given, together with a comparison with results by Nelson [4].

2. Diffusion-slowing down representation

Consider charged particle balance in differential space $d\boldsymbol{r}\ dE\ d\boldsymbol{\Omega}$ about position $\boldsymbol{r}$, energy E, and direction $\boldsymbol{\Omega}$. At steady state, by equating losses from leakage elastic collisions, slowing down by electronic interactions, and particle production; the following form

of the Boltzmann transport equation is obtained [5,6]:

$$\Omega \cdot \nabla \Phi(r, E, \Omega) + \Sigma_t(r, E, \Omega)\Phi(r, E, \Omega) = \frac{\partial[S(E)\Phi(r, E, \Omega)]}{\partial E} + \int d\Omega' \int dE' \Sigma_s(r, E' \to E, \Omega' \to \Omega)\Phi(r, E, \Omega) + Q(r, E, \Omega), \quad (1)$$

where

$\Phi(r, E, \Omega)$ = particle angular flux
= (particle speed) × (particle number density);

$\Omega \cdot \nabla \Phi(r, E, \Omega)\, dr\, dE\, d\Omega$
= net rate at which particles are lost from $dr\, dE\, d\Omega$ due to leakage;

$\Sigma_t(E)$ = total macroscopic cross section;

$\Sigma_t(E)\Phi(r, E, \Omega)\, dr\, dE\, d\Omega$ = rate at which particle undergo nuclear interactions in $dr\, dE\, d\Omega$;

$\Sigma_s(E' \to E, \Omega' \to \Omega)$
= differential scattering cross section;

$\int d\Omega' \int dE' \Sigma_s(E' \to E, \Omega' \to \Omega)\phi(r, E', \Omega')]\, dr\, dE\, d\Omega$ = rate at which particles scatter into $dr\, dE\, d\Omega$;

$\frac{\partial[S(E)\Phi(r, E, \Omega)]}{\partial E} dr\, dE\, d\Omega$
= net rate at which particles slow down into $dr\, dE\, d\Omega$ due to Coulomb interactions with electrons;

$S(E)$ = electronic stopping cross section;

$Q(r, E, \Omega)$ = source for PKA's.

For charged particle transport problems such as the slowing down of PKA's in materials, scattering processes are due to nuclear as well as electronic interactions. Nuclear interactions occur mainly by screened Coulomb collisions between a moving atom and background atoms. Electronic interactions are of Coulomb type collisions between moving atoms and the background electron cloud. Due to the fact that electronic collisions are highly forward, we were able to replace the electronic inscattering integral in the transport equation by substituting an electronic stopping term for the integral in the transport eq. (1).

The previous transport equation has six degrees of freedom; namely, three spatial, one energy and the remainder from velocity direction cosine dependence. Assuming that the angular flux has nearly isotropic distribution, diffusion equations can be derived from the transport equation. Such simplication leads to the elimination of two independent variables (velocity direction cosines) and the reduction of degrees of freedom from 6 to 4. Computer simulations have shown that displacement collisions are isotropic in cascades over most of the energy range. Also PKA sources have isotropic and homogeneous distributions. We will therefore use the simpler diffusion approximation in our attempt to calculate a dissolution parameter. The only independent variables in these equations are space and energy. In order to simplify mathematics, and for the sake of obtaining approximate analytical solutions, we will assume that nuclear scattering is approximately isotropic. However, electronic stopping is highly anisotropic, and we will take account of this by using an average scattering cosine of unity for electronic stopping. Since the PKA source is spatially isotropic, the error in the assumption of isotropic nuclear scattering is expected to be very small, as is the case in neutron transport calculations [7]. The diffusion approximation has the following expression, where the angular dependence is eliminated from the transport formulation:

$$J(r, E) = -\frac{1}{3\Sigma_t} \nabla \Phi(r, E) = -D \nabla \Phi(r, E), \quad (2)$$

where D is the diffusion coefficient, and Σ_t is the total cross section.

$D = 1/3\Sigma_t$.

By integrating eq. (1) over $d\Omega$ and substituting eq. (2), we obtain

$$-D\nabla^2\Phi + \Sigma_t\Phi = Q + \frac{d}{dE}(S\Phi) + \int_0^\infty dE' \Sigma_s(E' \to E)\Phi(r, E'), \quad (3)$$

where ∇^2 describes spatial diffusion, J is the energy current and Φ is the energy flux.

This equation is strictly valid for monoatomic homogeneous media. For an inhomogeneous polyatomic medium, coupled diffusion equations must be used. Let us consider a precipitate embedded in an infinite matrix, an example is the carbide precipitate $M_{23}C_6$ in steel. In order to simplify the treatment, an average atom type will be used to represent the two types of atoms, M and C, in the precipitate. Furthermore, we expand the self atom inscattering term into deflected and recoil terms. We also separate the recoil terms due to atoms coming from different spatial regions from those due to self atoms. With this coupling between different atomic species and different spatial regions, the analytical solution of eq. (3) is still a difficult task. We will invoke here one more assumption for the sake of simplicity, and that is to render the electronic energy loss rate zero, but subsume its effect in a modified diffusion length as evaluated from the Monte Carlo range calculations. The coupled diffusion equations for a precipitate in an infinite matrix are then given below

$$-D_{pp}\nabla^2\Phi_p + \Sigma_{tpp}\Phi_p = \int \Sigma_{spp}(E' \to E)\Phi_p(E')\, dE' + \int \Sigma_{spp}(E' \to E' - E)\Phi_p(E')\, dE' + \int \Sigma_{spm}(E' \to E' - E)\Phi_m(E')\, dE' + S_p(E), \quad (4)$$

$$-D_{pm}\nabla^2\Phi_m+\Sigma_{tpm}\Phi_m=\int\Sigma_{spm}(E'\to E)\Phi_m(E')\,dE', \tag{5}$$

$$-D_{mp}\nabla^2\Phi_p+\Sigma_{tmp}\Phi_p=\int\Sigma_{smp}(E'\to E)\Phi_p(E')\,dE', \tag{6}$$

$$\begin{aligned}-D_{mm}\nabla^2\Phi_m+\Sigma_{tmm}\Phi_m&=\int\Sigma_{smm}(E'\to E)\Phi_m(E')\,dE'\\&\quad+\int\Sigma_{smm}(E'\to E'-E)\Phi_m(E')\,dE'\\&\quad+\int\Sigma_{smp}(E'\to E'-E)\Phi_p(E')\,dE'+S_m(E).\end{aligned} \tag{7}$$

Two subscripts are used for physical parameters in eqs. (4)–(7). "p" stands for precipitate and "m" for matrix. The first subscript depicts the region where the equation is valid and the second subscript represents the atom type being studied. Eq. (4) is for the diffusion of precipitate atoms in the precipitate, Eq. (5) is for the diffusion of matrix atoms in the precipitate, eq. (6) is for precipitate atoms in the matrix, and eq. (7) is for matrix atoms in the matrix. Eqs. (5) and (6) cannot be neglected due to the fact that foreign recoils in the local medium do contribute greatly to the generation of local recoils around the interface. Four boundary conditions are required to solve for either matrix or precipitate atom fluxes; these are:

$$\Phi(\infty)=\text{finite}, \tag{8}$$

$$\Phi(\boldsymbol{r}_b)=\Phi(\boldsymbol{r}_b), \tag{9}$$

$$\boldsymbol{J}(\boldsymbol{r}_b)=\boldsymbol{J}(\boldsymbol{r}_b), \tag{10}$$

$$\boldsymbol{J}(0)=0, \tag{11}$$

where $\boldsymbol{r}_b$ is a vector defining the microstructure surface.

If the mass of precipitate atoms is drastically different from matrix atoms, as is the general case, this can lead to different slowing down behaviors for these atoms. In order to consider mass differences among the interacting particles, slowing down energy ranges will have to be modified and the solution is more complex, as is the case for neutron slowing down in non-hydrogenous media (referred to as Plazec's wiggle) [8]. A good measure for the mass disparity among interacting particles is the kinetic energy transfer factor, A, which describes the maximum fraction of energy that an incident particle of mass M_1 can transfer to a recoil particle with mass M_2. It is defined as

$$A=\frac{4M_1M_2}{(M_1+M_2)^2} \tag{12}$$

if the masses are the same, A is unity, and if the masses are drastically different, A approaches zero. Also, α, the minimum fraction of energy that an incident particle can emerge with after a collision, is given as

$$\alpha=1-A=\left(\frac{M_1-M_2}{M_1+M_2}\right)^2. \tag{13}$$

This factor affects the slowing down energy range; if α equals zero an incident particle can lose all of its energy in a single collision, while for the case α approaches unity it needs a large number of collisions before the incident particle can be slowed down to a small energy. Fortunately, for the case of precipitate $M_{23}C_6$, such a pure molybdenum carbide, in steel, the average mass of precipitate atoms is about 1.5 times that of iron atoms. This gives a A of 0.97 and an α of 0.03. These two parameters are very close to those of the case when precipitate and steel atom have the same mass. Therefore, we can use the formulation of equal masses for this analysis. This can considerably simplify the problem as what is faced in neutron slowing down problem [8].

3. Method of solution: Neumann expansion

We can solve the coupled diffusion equations by expanding the energy fluxes for precipitate and matrix atoms into a Neumann series of the following form

$$\Phi(\boldsymbol{r},E)=\sum_{n=0}^{\infty}\Phi_n(\boldsymbol{r},E), \tag{14}$$

where Φ_n is the successive corrections to the zeroth order solution. Each term in the Neumann series expansion has the analogy of collided flux as from transport equations. By applying a Neumann expansion for the fluxes, we can decouple the inscattering integral from the spatial dependence terms. However, a new series of diffusion equations arise as shown below

zeroth order equations:

$$-D_{pp}\nabla^2\Phi_{p,0}+\Sigma_{tpp}\Phi_{p,0}=S_p(E), \tag{15}$$

$$-D_{pm}\nabla^2\Phi_{m,0}+\Sigma_{tpm}\Phi_{m,0}=0, \tag{16}$$

$$-D_{mp}\nabla^2\Phi_{p,0}+\Sigma_{tmp}\Phi_{p,0}=0, \tag{17}$$

$$-D_{mm}\nabla^2\Phi_{m,0}+\Sigma_{tmm}\Phi_{m,0}=S_m(E). \tag{18}$$

first order and higher ($n\geqslant 1$):

$$\begin{aligned}-D_{pp}\nabla^2\Phi_{p,n}+\Sigma_{tpp}\Phi_{p,n}&=\int\Sigma_{spp}(E'\to E)\Phi_{p,n-1}(E')\,dE'\\&\quad+\int\Sigma_{spp}(E'\to E'-E)\Phi_{p,n-1}(E')\,dE'\\&\quad+\int\Sigma_{spm}(E'\to E'-E)\Phi_{m,n-1}(E')\,dE',\end{aligned} \tag{19}$$

$$-D_{pm}\nabla^2\Phi_{m,n}+\Sigma_{tpm}\Phi_{m,n}=\int\Sigma_{spm}(E'\to E)\Phi_{m,n-1}(E')\,dE', \tag{20}$$

$$-D_{mp}\nabla^2\Phi_{p,n}+\Sigma_{tmp}\Phi_{p,n}$$
$$=\int\Sigma_{smp}(E'\to E)\,\Phi_{p,n-1}(E')\,dE', \tag{21}$$
$$-D_{mm}\nabla^2\Phi_{m,n}+\Sigma_{tmm}\Phi_{m,n}$$
$$=\int\Sigma_{smm}(E'\to E)\,\Phi_{m,n-1}(E')\,dE'$$
$$+\int\Sigma_{smm}(E'\to E'-E)\,\Phi_{m,n-1}(E')\,dE'$$
$$+\int\Sigma_{smp}(E'\to E'-E)\,\Phi_{p,n-1}(E')\,dE', \tag{22}$$

with the boundary conditions (8–11) applied to each flux component.

In the present analysis, two different geometries for precipitate shapes are considered; namely, plane and spherical, with the corresponding appropriate expression for the operator ∇^2. The operator for spherical geometry causes some difficulties. By a change of variable such as:

$$\Phi=\Psi/r, \tag{23}$$

we obtain similar diffusion equations to those of the planar case with Ψ in place of Φ. However, the external PKA source term is rQ for spherical geometry rather than Q as for plane geometry.

The solution to the previous set of equations still requires a numerical approach, if complicated nuclear scattering cross-sections are used. Our major objective is to obtain a simple analytical approximation, rather than involved numerical calculations. For this purpose, we will assume the existence of an "equivalent" hard sphere cross-section, that is valid over the entire energy range. It is known that the interaction potential goes from nearly pure Coulomb scattering at high energy to a Born–Meyer type interaction potential at low energies. In our simplified analysis, the "equivalent" hard-sphere cross-section is only a model of the entire interaction range. The value of this cross-section is determined such that the atomic displacement rate is normalised to the more sophisticated Monte Carlo numerical simulations of our code TRIPOS [3]. Hence, the results of the present calculations give only "relative" values of dissolution to displacement rates.

For hard sphere nuclear scattering, we have

$$\Sigma_s(E'\to E)=\Sigma_s(E')/E'. \tag{24}$$

Also in the process of slowing down for PKA's, the total cross section is essentially the same as the scattering cross section, i.e., $\Sigma_s=\Sigma_t$, until the energy falls below a certain energy limit when the slowing down process is terminated and the particle is considered to be absorbed. Also from the fact that precipitate atoms have similar masses and atomic numbers as those of matrix atoms, it follows that they have similar atomic scattering and diffusional behaviors. Therefore, we have

$$\Sigma=\Sigma_{tpp}=\Sigma_{tpm}=\Sigma_{tmp}=\Sigma_{tmm}=\Sigma_{spp}=\Sigma_{spm}$$
$$=\Sigma_{smp}=\Sigma_{smm} \tag{25}$$

and

$$D=D_{pp}=D_{pm}=D_{mp}=D_{mm}. \tag{26}$$

Eqs. (19) to (22) can be further simplified by combining the deflected and recoil inscattering terms for self atoms. The simplified diffusion slowing down equations are for $n\geqslant 1$:

in precipitate:

$$-D\nabla^2\Phi_{p,n}+\Sigma\Phi_{p,n}$$
$$=2\int\frac{\Sigma(r,E')\Phi_{p,n-1}(r,E')\,dE'}{E'}$$
$$+\int\frac{\Sigma(r,E')\Phi_{m,n-1}(r,E')\,dE'}{E'}, \tag{27}$$
$$-D\nabla^2\Phi_{m,n}+\Sigma\Phi_{m,n}$$
$$=\int\frac{\Sigma(r,E')\Phi_{m,n-1}(r,E')\,dE'}{E'}; \tag{28}$$

in matrix:

$$-D\nabla^2\Phi_{p,n}+\Sigma\Phi_{p,n}=\int\frac{\Sigma(r,E')\Phi_{p,n-1}(r,E')\,dE'}{E'} \tag{29}$$
$$-D\nabla^2\Phi_{m,n}+\Sigma\Phi_{m,n}$$
$$=2\int\frac{\Sigma(r,E')\Phi_{m,n-1}(r,E')\,dE'}{E'}$$
$$+\int\frac{\Sigma(r,E')\Phi_{p,n-1}(r,E')\,dE'}{E'}. \tag{30}$$

For $n=0$, we do not have the inscattering terms on the right hand side. However, we have a precipitate source term for eq. (27) and matrix source term for eq. (30).

Let all the PKA's start with energy E_0, using the following transformations,

$$y=r/L, \tag{31}$$
$$\epsilon=E/E_0, \tag{32}$$

where $L=\sqrt{D/\Sigma}$ is the diffusion length, E_0 is the PKA source energy. Eqs. (27)–(30) can be rewritten as below (for plane geometry) in dimensionless units, for $n\geqslant 1$:

$$-\nabla_y^2\Phi_{p,n}(y,\epsilon)+\Phi_{p,n}(y,\epsilon)$$
$$=2\int_\epsilon^1\frac{\Phi_{p,n-1}(y,\epsilon')}{\epsilon'}\,d\epsilon'+\int_\epsilon^1\frac{\Phi_{m,n-1}(y,\epsilon')}{\epsilon'}\,d\epsilon', \tag{33}$$
$$-\nabla_y^2\Phi_{m,n}(y,\epsilon)+\Phi_{m,n}(y,\epsilon)$$
$$=\int_\epsilon^1\frac{\Phi_{m,n-1}(y,\epsilon')}{\epsilon'}\,d\epsilon', \tag{34}$$

$$-\nabla_y^2\Phi_{p,n}(y,\epsilon)+\Phi_{p,n}(y,\epsilon)=\int_\epsilon^1\frac{\Phi_{p,n-1}(y,\epsilon')}{\epsilon'}\,d\epsilon', \tag{35}$$

$$-\nabla_y^2\Phi_{m,n}(y,\epsilon)+\Phi_{m,n}(y,\epsilon)=2\int_\epsilon^1\frac{\Phi_{m,n-1}(y,\epsilon')}{\epsilon'}\,d\epsilon'+\int_\epsilon^1\frac{\Phi_{p,n-1}(y,\epsilon')}{\epsilon'}\,d\epsilon'. \tag{36}$$

For $n=0$, again we do not have the inscattering terms on the right hand side of the above four equations, however precipitate source and matrix source terms do exist on the right hand side of eqs. (33) and (36), respectively. The following solutions are obtained for plane and spherical geometries, when the ∇^2 operator is replaced by its appropriate representation.

For plane geometry:

$$\Phi_{p,0}=\left(d_{p,0}+a_{p,0,0}e^{-y}+b_{p,0,0}e^{y}\right)\delta(\epsilon-1), \tag{37}$$

$$\Phi_{m,0}=\left(a_{m,0,0}e^{-y}+b_{m,0,0}e^{y}\right)\delta(\epsilon-1), \tag{38}$$

$$\Phi_{p,0}=c_{p,0,0}e^{-y}\delta(\epsilon-1), \tag{39}$$

$$\Phi_{m,0}=\left(d_{m,0}+c_{m,0,0}e^{-y}\right)\delta(\epsilon-1); \tag{40}$$

while for $n>0$, the following solution is obtained:

$$\Phi_{p,n}=\left[d_{p,n}+\sum_{k=0}^{n}\left(a_{p,n,k}e^{-y}+b_{p,n,k}e^{y}\right)y^k\right]\times\ln^{n-1}(1/\epsilon), \tag{41}$$

$$\Phi_{m,n}=\sum_{k=0}^{n}\left(a_{p,n,k}e^{-y}+b_{p,n,k}e^{y}\right)y^k\ln^{n-1}(1/\epsilon), \tag{42}$$

$$\Phi_{p,n}=\sum_{k=0}^{n}c_{p,n,k}e^{-y}y^k\ln^{n-1}(1/\epsilon), \tag{43}$$

$$\Phi_{m,n}=\left[d_{m,n}+\sum_{k=0}^{n}c_{m,n,k}e^{-y}y^k\right]\ln^{n-1}(1/\epsilon). \tag{44}$$

The solution coefficients, a, b, c and d, for both plane and spherical geometries, are given in appendix A.

The total precipitate and matrix atom fluxes and currents are the sum of component fluxes and currents for each type over the whole PKA slowing down energy regime, as defined in eq. (14).

$$\Phi_{Tot}(\boldsymbol{r})=\int\Phi(\boldsymbol{r},E')\,dE'=\sum_{n=0}^{\infty}\int\Phi_n(\boldsymbol{r},E')\,dE', \tag{45}$$

$$J_{Tot}(\boldsymbol{r})=\int\boldsymbol{J}(\boldsymbol{r},E')\,dE'=\sum_{n=0}^{\infty}\int\boldsymbol{J}_n(\boldsymbol{r},E')\,dE'. \tag{46}$$

The dissolution rate of the precipitate is proportional to the total precipitate atom current that crosses the precipitate surface. The dissolution parameter, b, can now be calculated as:

$$b=\frac{J_{Tot}A}{V}=\frac{3J_{Tot}}{r_{eq}}, \tag{47}$$

where V and A are the volumes and surface area for the precipitate and r_{eq} is the equivalent radius for the precipitate.

4. Results

In these calculations, we consider a precipitate of the $M_{23}C_6$ type and the steel matrix is considered to contain iron atoms only. Average atoms are used for the representation of precipitate atoms. In other words, an average mass and an average atomic number are used to characterize precipitate atoms. In the present method, it is not possible to calculate preferential dissolution rates of precipitate components, as has been accomplished using the Monte Carlo method [3]. Average PKA's are used in the solving down-diffusion theory of calculations. The cutoff energy is taken to be the bulk displacement energy which equals 25 eV. By solving the previous set of coupled equations, precipitate atom fluxes and matrix atom fluxes are obtained throughout the medium. Neumann series of up to 45 terms was found necessary before fluxes would converge.

Fig. 1 shows the flux profiles for both matrix and precipitate atoms for a plane precipitate with half thickness of 5 diffusion lengths. For the case considered, precipitate and matrix atoms are of similar masses, similar atomic numbers, and same source strength. The combined flux for precipitate and matrix atoms, that is, Φ_p and Φ_m is essentially the same as that for an infinite medium. For more detail on the flux in the infinite medium, the reader is referred to appendix B at the end

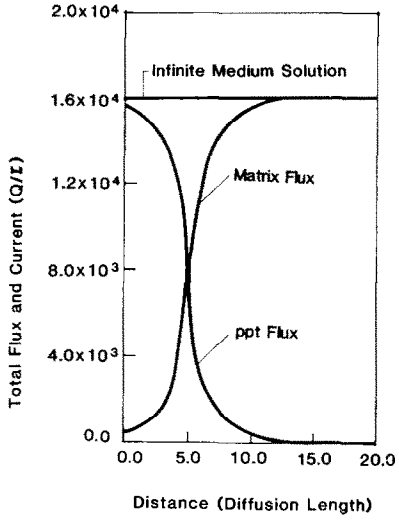

Fig. 1. Precipitate (ppt) and matrix fluxes as functions of distance from the center of a slab precipitate with half-thickness equal to 5 diffusion lengths. The sum of precipitate and matrix fluxes converges to the flux for an infinite medium.

of this paper. Fig. 1 illustrates that the sum of precipitate and matrix fluxes does converge to the infinite medium flux. Figs. 2 and 3 show the fluxes in Neumann series terms. Fig. 2 gives the 6th to the 10th term and fig. 3 gives the 31st to the 35th terms. A plane precipitate is considered for the above evaluations. However, it is known that generally precipitates have spherical shapes. Therefore a question arises regarding the validity of plane geometry calculations for spherical precipitates. An "effective radius" for a planar precipitate is calculated by conserving the volume to surface ratio of the precipitate. Let t equal half thickness of the planar precipitate, then the associated effective radius is $3t/2$. Fig. 4 shows a comparison of fluxes at the precipitate surface between plane and spherical geometries as functions of equivalent radii. It shows that for large sizes, precipitate fluxes for spherical and planar models are similar while for small sizes, precipitate fluxes for the spherical model are smaller than those for the planar models. However, the physical entity that depicts the dissolution processes is the current that crosses the precipitate surface. The dissolution parameter can be evaluated by using eq. (47) along with the current. The best way to represent the dissolution parameter is to express it as a fraction of the dpa rate. As we know, for very small precipitates, the dissolution rate is essentially equal to the dpa rate. The dissolution parameter can then be normalized to the dpa rate at very small radii. Fig. 5 shows a comparison of dissolution parameters between plane and spherical model. The results are

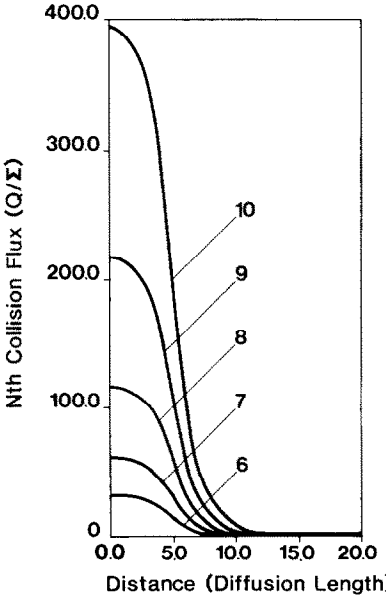

Fig. 2. 6th–10th Neumann expansion collision fluxes as functions of distance from the center of a slab precipitate with half-thickness equals to 5 diffusion lengths.

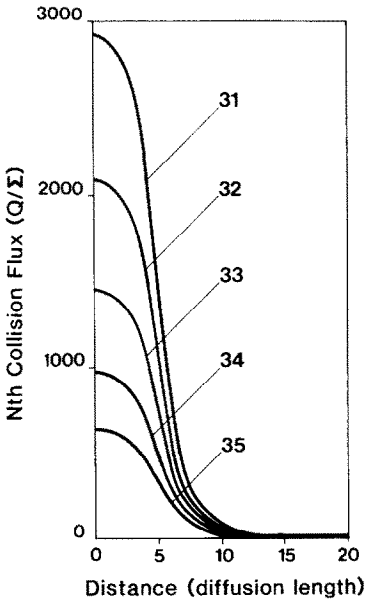

Fig. 3. 31st–35th Neumann expansion collision fluxes as functions of distance from the center of a slab precipitate with half-thickness equals to 5 diffusion lengths.

about the same for large and small radii and within a difference of 20% for intermediate radii.

In the five figures above, the distance is expressed in units of diffusion length. In order to make the results have experimental significance, it is necessary to measure and convert the diffusion length into real units. A rule of thumb for the diffusion length is that it is about one seventh to one sixth that of the PKA ranges. Our

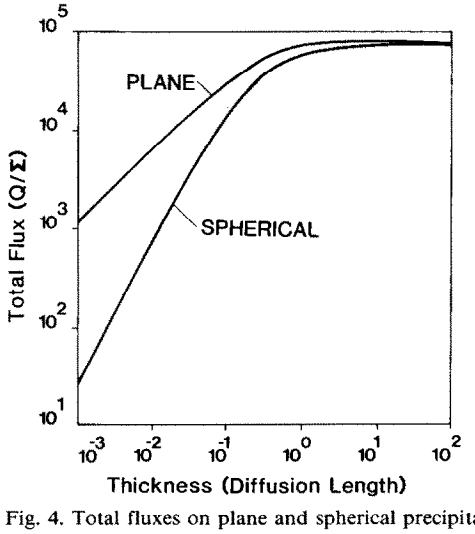

Fig. 4. Total fluxes on plane and spherical precipitate surfaces as functions of equivalent precipitate thickness in diffusion lengths.

earlier work on the contribution of direct dissolution from the self collision cascade has shown that the direct dissolution parameters peaks for planar precipitate with half thickness corresponding to 6–7 diffusion lengths. The peak corresponds to the ranges of PKA's. Furthermore, expansions for Neumann series of up to about 40 terms are required for the flux calculation to reach convergence. This suggests that it takes about 40 collisions for PKA to slow down if we remember that the nth term in the Neumann series expansion in diffusion theory corresponds to the nth collided term from transport theory. This also suggests that 6–7 diffusion lengths correspond to the range of a PKA from random work theory. That is, the square of the travel distance is equal to the number of jumps (collisions) times the square of the jump step (diffusion length). We have therefore taken the diffusion lengths as 1/6.5 of the ranges of PKA's. The ranges of those PKA's are calculated by using the Monte Carlo computing program, TRIPOS.

Fig. 5 shows the dissolution rate as a function of the equivalent precipitate radius. PKA's at different energies have the same slowing down behavior. A group of dissolution parameter curves can be obtained by using the real units in place of diffusion lengths for PKA's at different energies, fig. 6. The figure shows five curves from left to right with PKA energies of 1 keV, 10 keV, 37 keV, 0.2 MeV, and 0.5 MeV, respectively. By examination of the dissolution parameters plotted on log–log scales as in fig. 7, it can be observed that the plot has two asymptotic limits, one with zero slope for small precipitates and the other with a negative slope. The intersection of those two asymptotic lines is at an equivalent radius of about 0.6 diffusion length. The ranges of PKA's at different energies calculated by using TRIPOS for Fe on Fe can be approximated by

$$R(\text{range}) = 5.3[E(\text{keV})]^{0.911}, \tag{48}$$

where R is in the units of ångströms and E is the average PKA energy. This expression has been found to be valid in the energy range of 1 keV to 500 keV. And the diffusion length is therefore given by

$$L = R(\text{range})/6.5 = 0.815E^{0.911}. \tag{49}$$

The dissolution parameter, b, can then be empirically found to be

$$\begin{aligned} b &\simeq 1 \qquad r < 0.6L, \\ &\simeq \frac{E^{0.911}}{2r_b} \qquad r > 0.6L, \end{aligned} \tag{50}$$

where r_b is the radius of the precipitate in ångströms and E is the PKA energy in keV. The "escape zone" concept proposed by Nelson [4] for resolution of fission gas bubbles in fission environments has the expression

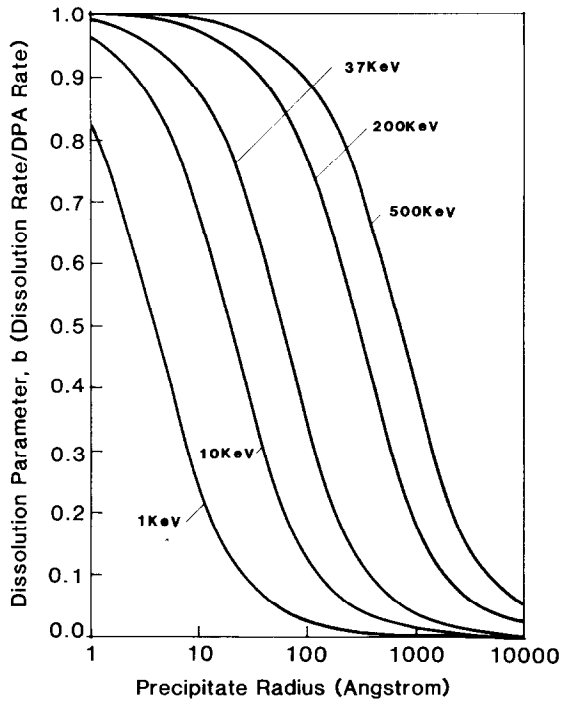

Fig. 6. Dissolution parameters for different PKA energies as a function of precipitate radius in ångströms.

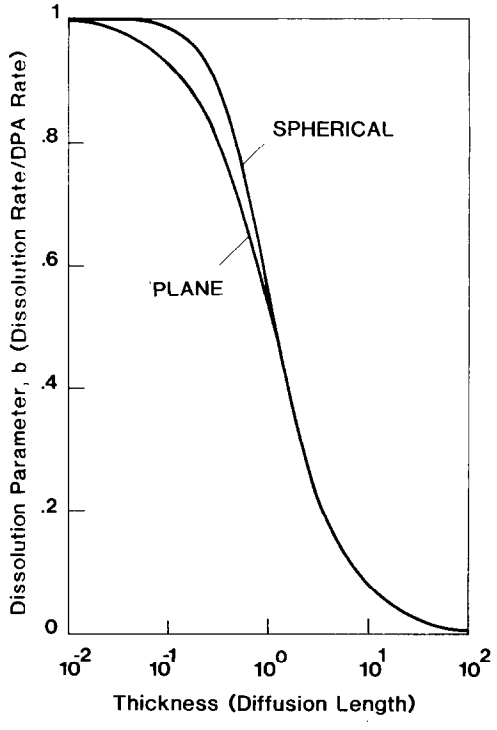

Fig. 5. Dissolution parameters for plane and spherical precipitates as functions of equivalent precipitate thickness in diffusion lengths.

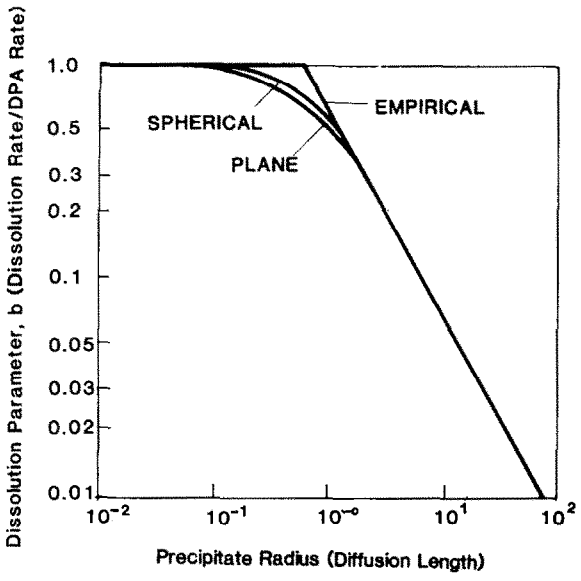

Fig. 7. Empirical dissolution parameter compared with dissolution parameters for spherical and plane precipitates as a function of equivalent radius in diffusion lengths.

as below,

$$b = 1 \qquad r_b < d,$$
$$= \frac{r_b^3 - (r_b - d)^3}{r_b^3} \qquad r_b > d, \tag{51}$$

where r_b is the bubble radius and d is an empirical escape distance on the order of 15 Å.

By examination of eqs. (50) and (51), it is shown that the original Nelson concept [4] of an "escape-zone" for fission gas bubbles can now be extended to precipitate dissolution. The dissolution rate is approximately linear with incident PKA energy and inversely proportional to the precipitate radius.

Appendix A: Solution constants

The constants a, b, c and d in the Neumann series expansion can be solved by using the boundary conditions as well as the recursive relationship. In table 1, solution constants for the zeroth Neumann expansion are given for both planar and spherical geometries. For higher order Neumann series expansion, the recursive relationships are given as below.

$$d_{p,n} = 2d_{p,n-1}/(n-1), \tag{A.1}$$
$$a_{p,n,n} = \left(a_{p,n-1,n-1} + a_{m,n-1,n-1}/2\right)/n(n-1), \tag{A.2}$$
$$b_{p,n,n} = \left(b_{p,n-1,n-1} + b_{m,n-1,n-1}/2\right)/n(n-1), \tag{A.3}$$
$$c_{p,n,n} = c_{p,n-1,n-1}/2n(n-1), \tag{A.4}$$
$$d_{m,n} = 2d_{m,n-1}/(n-1), \tag{A.5}$$
$$a_{m,n,n} = a_{m,n-1,n-1}/2n(n-1), \tag{A.6}$$
$$b_{m,n,n} = b_{m,n-1,n-1}/2n(n-1), \tag{A.7}$$
$$c_{m,n,n} = \left(c_{m,n-1,n-1} + c_{p,n-1,n-1}/2\right)/n(n-1), \tag{A.8}$$

for $k < n$

$$a_{p,n,k} = \left(a_{p,n-1,k-1} + a_{m,n-1,k-1}/2\right)/k(n-1) + \frac{k+1}{2} a_{p,n,k+1}, \tag{A.9}$$
$$b_{p,n,k} = \left(b_{p,n-1,k-1} + b_{m,n-1,k-1}/2\right)/k(n-1) + \frac{k+1}{2} b_{p,n,k+1}, \tag{A.10}$$
$$c_{p,n,k} = c_{p,n-1,k-1}/2k(n-1) + \frac{k+1}{2} c_{p,n-1,k-1}, \tag{A.11}$$
$$a_{m,n,k} = a_{m,n-1,k-1}/2k(n-1) + \frac{k+1}{2} a_{m,n,k+1}, \tag{A.12}$$
$$b_{m,n,k} = b_{m,n-1,k-1}/2k(n-1) + \frac{k+1}{2} b_{m,n,k+1}. \tag{A.13}$$

Table 1
Solution constants for zeroth Neumann solution

	Plane geometry	Spherical geometry
$a_{p,0,0}$	$0.5\exp(-y_b)Q_p$	$0.5(1+y_b)\exp(-y_b)Q_m$
$a_{m,0,0}$	$-0.5\exp(-y_b)Q_m$	$-0.5(1+y_b)\exp(-y_b)Q_p$
$b_{p,0,0}$	$a_{p,0,0}$	$-a_{p,0,0}$
$b_{m,0,0}$	$a_{m,0,0}$	$-a_{m,0,0}$
$c_{p,0,0}$	$0.5Q_p(\exp(-y_b)-\exp(y_b)$	$0.50Q_p(1+y_b)(\exp(-y_b)+\exp(y_b)$
$c_{m,0,0}$	$0.5Q_m(\exp(y_b)-\exp(-y_b))$	$-0.5Q_m(1+y_b)(\exp(-y_b)+\exp(y_b))$
$d_{p,0}$	Q_p	y_bQ_p
$d_{m,0}$	Q_m	y_bQ_m

y_b is the radius (half thickness) of the precipitate.

$$c_{m,n,k} = \left(c_{m,n-1,k-1} + c_{p,n-1,k-1}/2\right)/k(n-1) + \frac{k+1}{2} a_{m,n,k+1}, \tag{A.14}$$

Appendix B: Flux in an infinite medium

For the case of cascade slowing down in an infinite medium, there is no space diffusion term. Therefore we have

$$\Sigma_t(E)\phi(E) = 2\int \Sigma_s(E' \to E)\phi(E')\,dE' + Q\delta(E - E_0), \tag{B.1}$$

where the dependence on r has been removed. Let us assume constant cross-sections and hard sphere scattering, we then have

$$\Sigma_s(E) = \Sigma_t(E) = \Sigma, \tag{B.2}$$

$$\Sigma_s(E' \to E) = \Sigma_s(E')/E' = \Sigma/E'. \tag{B.3}$$

Eq. (B.1) can be rewritten as

$$\Sigma\phi(E) = 2\int_E^{E_0} \frac{\Sigma\phi(E')\,dE'}{E'} + Q\delta(E - E_0). \tag{B.4}$$

Let $\Sigma\phi(E) = F(E)$. (B.5)

Again eq. (B.4) has the new form

$$F(E) = 2\int_E^{E_0} \frac{F(E')}{E'}\,dE' + Q\delta(E - E_0). \tag{B.6}$$

Define a new variable, $G(E)$, as

$$G(E) = F(E) + Q\delta(E - E_0), \tag{B.7a}$$

i.e.

$$F(E) = G(E) + Q\delta(E - E_0). \tag{B.7b}$$

Substitute eq. (B.7b) in eqs. (B.6), we have

$$G(E) = \frac{2Q}{E_0} + \int_E^{E_0} \frac{G(E')}{E'}\,dE'. \tag{B.8}$$

Equation (B.8) can be simplified by differentiating it with respect to E, we have

$$\frac{dG(E)}{dE} = -\frac{2G(E)}{E}. \tag{B.9}$$

The solution for eq. (B.9) is

$$G(E) = CE^{-2}. \tag{B.10}$$

by $G(E_0) = 2Q/E_0$, we know

$$C = 2QE_0 \tag{B.11}$$

therefore

$$\Sigma\phi(E) = \frac{2QE_0}{E^2} + Q\delta(E - E_0)$$
$$\phi(E) = \frac{2QE_0}{\Sigma E^2} + \frac{Q}{\Sigma}\delta(E - E_0). \tag{B.12}$$

Therefore, we know that $\phi(E)$ has a $1/E^2$ dependence for $E \leqslant E_0$. The total flux is

$$\phi_{\cdot\Gamma} = \int_{E_c}^{E_0} \phi(E)\,dE = \frac{2QE_0}{\Sigma E_c} - \frac{Q}{\Sigma} = \frac{2QE_0}{\Sigma E_c} \quad \text{if } E_0 > E_c. \tag{B.13}$$

This work is supported by the National Science Foundation Grant No. CPE 81-11571 at UCLA. The authors wish to thank Dr. A. Prinja for his critique of the manuscript.

References

[1] P. Wilkes, J. Nucl. Mater. 83 (1979) 66.
[2] R.S. Nelson, J.A. Hudson and D.J. Mazey, J. Nucl. Mater. 44 (1972) 318.
[3] P.S. Chou and N.M. Ghoniem, J. Nucl. Mater. 117 (1983) 55.
[4] R.S. Nelson, J. Nucl. Mater. 31 (1968) 153.
[5] D.E. Bartine, R.G. Alsmiller, F.R. Mynatt, W.W. Engle and J. Barish, Nucl. Sci. Eng. 48 (1972) 159.
[6] J.J. Hoffman, H.L. Dodds and D.K. Holmes, Nucl. Sci. Eng. 68 (1976) 204.
[7] G. Pomraning, UCLA, private communication.
[8] J.J. Duderstadt and L.J. Hamilton, Nuclear Reactor Analysis (Wiley, New York, 1976) p. 319.